Planning Shortest Bounded–Curvature Paths for a Class of Nonholonomic Vehicles among Obstacles

Antonio Bicchi
Giuseppe Casalino
Corrado Santilli

Dipartimento Sistemi Elettrici e Automazione
Università di Pisa
via Diotisalvi, 2 – 56100 Pisa – Italia

Fax: +39–50–565333 Tel.:+39–50–565328 Email: bicchi@vm.cnuce.cnr.it

Abstract

This paper deals with the problem of planning a path for a robot vehicle amidst obstacles. The kinematics of the vehicle being considered are of the unicycle or car–like type, i.e. are subject to nonholonomic constraints. Moreover, the trajectories of the robot are supposed not to exceed a given bound on curvature, that incorporates physical limitations of the allowable minimum turning radius for the vehicle. The method presented in this paper attempts at extending Reeds and Shepp's results on shortest paths of bounded curvature in absence of obstacles, to the case where obstacles are present in the workspace. The method does not require explicit construction of the configuration space, nor employs a preliminary phase of holonomic trajectory planning. Successfull outcomes of the proposed technique are paths consisting of a simple composition of Reeds/Shepp paths that solve the problem. For a particular vehicle shape, the path provided by the method, if regular, is also the shortest feasible path. In its original version, however, the method

may fail to find a path, even though one may exist. Most such empasses can be overcome by use of a few simple heuristics, discussed in the paper. Applications to both unicycle and car–like (bicycle) mobile robots of general shape are described and their performance and practicality discussed.

1 Introduction

In recent years, there has been a growing interest in motion planning for nonholonomic vehicles, motivated by both its relevance to applications (automated factories and highways, assisted parking maneuvering, etc.) and its theoretical challenges. One of the interesting features of this field is that its background is composed of work done in holonomic motion planning (a predominantly A.I. area) as well as in nonlinear systems theory and control.

A nonholonomic constraint is a non integrable equation involving the configuration parameters and their derivatives (velocity parameters). Such constraints do not reduce the dimension of the robot configuration space (like holonomic constraints do), but reduce the dimension of the velocity space at any given configuration. Thus, a kinematic model of a car–like vehicle can be parked everywhere in a free three–dimensional workspace, although it only possesses two control inputs. This comes at the price of more complex planning for maneuvers such as parallel parking. Application of nonlinear control tools to nonholonomic planning generated elegant methods for steering robots between arbitrary configurations, e.g. by using sinusoidal [Murray and Sastry, 1993], or multirate [Monaco and Normand–Cyrot, 1992] control inputs. Although these methods do not consider the presence of obstacles nor bounds on curvatures, they provide a theoretically sound basis for generalizing local planning techniques (e.g. potential fields) to nonholonomic systems. In the case that obstacles are present, it has been shown (see Laumond [1986], Barraquand and Latombe [1990]) the non–trivial fact that a car with curvature limitations moving amidst obstacles remains fully controllable, that is, whenever a free (holonomic) trajectory exists, the existence of a feasible path is also guaranteed.

The presence of lower bounds on the minimum turning radius involves curvature constraints on feasible trajectories that deeply affect the geometry of the problem. The problem of finding the shortest path between two configurations in the plane with curvature limitations is an interesting ge-

ometric problem *per se*, that was solved first by Dubins [1957] for smooth trajectories. Only recently, Reeds and Shepp [1990] solved the geodesic problem when reversals are allowed. They have shown that a path with shortest length can always be built by concatenating at most five linear or circular segments, including at most two cusps. The radius of circular segments is the minimum allowed turning radius, and cusps correspond to reversals. The same result has recently been derived again by Sussmann and Tang [1991] and Boissonnat, Cerezo, and Leblond [1992], using Pontryagin's maximum principle. These theoretical results ignited a new series of methods tending to find nonholonomic paths with bounded curvature amidst obstacles, among which [Fortune and Wilfong, 1988], [Jacobs and Canny, 1989], [Barraquand and Latombe, 1989], [Jacobs, Laumond, Taix and Murray, 1991], [Mirtich and Canny, 1992].

The method presented in this paper is also inspired by Reeds and Shepp's work, and is reminiscent of several others proposed in the literature as well, though it does not seem to have been discussed in this form for nonholonomic vehicles. In particular, the method can be regarded as a generalization of visibility graph methods, to which it reduces as bounds on path curvature are lifted. The path resulting is a simple concatenation of linear and circular segments, the latter having minimum turning radii. For a special type of nonholonomic vehicle (a circular unicycle of radius h and minimum turning radius $\rho_{min} \leq h$) moving among polygonal obstacles, it is proved (Theorem 1) that, if the proposed planner succeeds in providing a regular path (i.e., a path with no cusps), then that is a shortest feasible path of bounded curvature for the given problem.

Although the method is not path–complete, a set of a few simple heuristics are presented that are generally capable of fixing most typical deadlocks of the algorithm. As applied to more general vehicles, the principal worth retained by the method is perhaps in its simplicity and in the smoothness of the resulting paths. The planner does not require explicit evaluation of the configuration space, nor it employs a preliminary phase of holonomic trajectory planning. Simulation results are reported in this paper that support such an extension providing very reasonable paths. Experiments have also been carried out on a TRC Inc. LABMATE vehicle, that showed the feasibility of real–time implementations of the algorithm in medium–complexity environments.

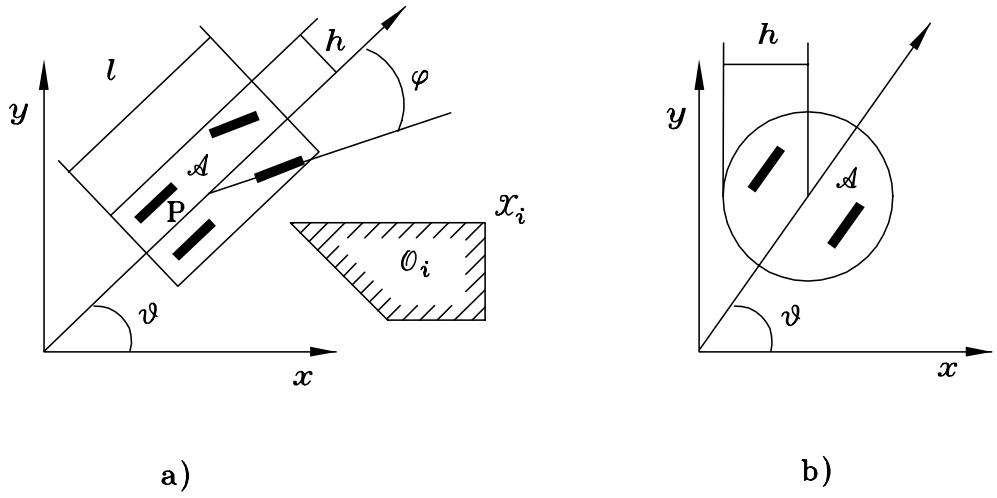

Figure 1: A generic car–like robot (a) and a particular unicycle vehicle (b).

2 The proposed planner

Fig.1–a shows a mobile robot, modelled as a two dimensional object $\mathcal{A}$ moving in a 2–dimensional workspace.

The configuration space of the robot is $\mathbf{R}^2 \times \mathbf{S}^1$, and can be parameterized by the coordinates x and y of the robot reference point P, and by the angle θ (representing the robot orientation) between the x–axis of the base frame $\mathcal{F}_S$ and the main axis of the robot. The robot shape is assumed symmetric with respect to its main axis, and its half-width is denoted by h. We restrict ourselves to consider only polygonal obstacles in the workspace, that we indicate with $\mathcal{O}_i$, $i = 1, \ldots, l$, while their n vertices are listed in $\mathcal{X}_j$, for $j = 0$ to n. A nonholonomic constraint arises because the wheels can roll and spin but not slip, hence the robot cannot move sidewise. For a unicycle vehicle such as that shown in fig.1–b, the nonholonomic constraint is written as

$$S(\mathbf{q})\dot{\mathbf{q}} = \left[\begin{array}{ccc} -\sin(\theta) & \cos(\theta) & 0 \end{array} \right] \left[\begin{array}{c} \dot{\mathbf{x}} \\ \dot{\mathbf{y}} \\ \dot{\theta} \end{array} \right] = 0$$

The motion planning problem can be stated as follows:

Problem 1 *Let* $\mathbf{q}_s = (x_s, y_s, \theta_s)$ *and* $\mathbf{q}_g = (x_g, y_g, \theta_g)$ *be respectively the initial and final configuration of a robot* $\mathcal{A}$ *with minimum turning radius* ρ_{min} *and half-width* h. *Determine a path* $\bar{\mathbf{q}}(\tau)$ *that minimizes the cost functional*

$$L(\bar{\mathbf{q}}(\cdot)) \stackrel{def}{=} \int_0^1 \sqrt{\mathbf{x}'^2(\lambda) + \mathbf{y}'^2(\lambda)}\; d\lambda, \tag{1}$$

subject to

$$\begin{aligned}
\bar{\mathbf{q}}(0) &= \mathbf{q}_s; && (2)\\
\bar{\mathbf{q}}(1) &= \mathbf{q}_g; && (3)\\
\mathcal{A}\left(\bar{\mathbf{q}}(\tau)\right) \cap \mathcal{O}_i &= \emptyset \;\; i = 1, \ldots, l, \;\; \forall \tau \in [0,1]; && (4)\\
S(\bar{\mathbf{q}})\bar{\mathbf{q}}' &= 0, \;\; \forall \tau \in [0,1]; && (5)\\
\bar{\mathbf{q}}(\tau) \in C^1, \text{ and } \frac{x'y'' - x''y'}{(x'^2 + y'^2)^{3/2}} &\leq \frac{1}{\rho_{min}}, && (6)
\end{aligned}$$

where $\bar{\mathbf{q}}' = \frac{d\bar{\mathbf{q}}(\tau)}{d\tau}$, $x' = \frac{dx(\tau)}{d\tau}$, $y' = \frac{dy(\tau)}{d\tau}$, $x'' = \frac{d^2x(\tau)}{d\tau^2}$, $y'' = \frac{d^2y(\tau)}{d\tau^2}$. In the above formulation, the cost functional is the length of the path, constraints (2) and (3) concern initial and final conditions of the path, condition (4) reflects the obstacle avoidance condition, while (5) and (6) represent the nonholonomic and limited curvature constraints on the path, respectively. Finding a solution for this problem is in general quite difficult. One possible approach to the study of such optimization problem is through Pontryagin's "Minimum Principle" [Pontryagin *et al.*, 1962]. However, as it is well known, the minimum principle only offers necessary conditions for the existence of an optimum solution in general. Moreover, constraints (4) are actually bounds on the state–space, and these entail a substantial increase in the complicacy of the analytical formulation of solutions to the problem above (see e.g. [Bryson and Ho, 1975]). In this paper, rather than pursuing such approach, we follow a constructive way of proving the optimal properties of a particular class of paths, which is described in the following algorithm.

Planner Algorithm.

a) *Draw* n *circles with radius* $\rho = \max\{\rho_{min}, h\}$ *centered in the vertices of the obstacles. Also draw two circles with radius* ρ_{min} *passing through* $[x_s,\ y_s]$ *and tangent to the line through* $[x_s,\ y_s]$ *with angle* θ_s, *and an analogous pair of circles for the final configuration* $\mathbf{q}_g$.

b) *Consider the $n+4$ circles two at a time, and draw the four linear segments belonging to the common tangent lines and comprised between the tangency points. Also consider all arcs on circles that join any two tangency points. Let a basic path diagram (BPD) be composed of two directed segments for each of these linear and circular segments.*

c) *The basic path diagram may contain non–free paths, that is, paths that cannot be followed by the robot without colliding with obstacles. Directed segments are then tested singularly and those causing collisions are eliminated from the diagram. In general, a segment may be free if followed in one sense, but not otherwise. For robots that are simmetric with respect to a line through the reference point and normal to the main axis of the robot, the direction of motion along a path is not relevant, and a simpler basic path diagram can be considered.*

d) *A directed graph G is built from the thus emended path diagram (EPD) as follows:*

- *the start and goal configurations are nodes of G;*
- *for all points of tangency between a linear and a circular segment, two configurations (corresponding to the possible orientations aligned with the common tangent direction) are nodes of G;*
- *two nodes i and j of G are connected with an oriented link from i to j if the corresponding directed segment on the emended path diagram exists;*
- *a cost equal to the length of the corresponding segment is associated to each link.*

e) *The directed graph G is searched for a path from the start to the goal configuration using the length of the overall path as the cost function.*

The above mentioned property of this planner is formalized in the following

Theorem 1 *For a circular mobile robot $\mathcal{A}$ with radius h equal to the minimum turning radius ρ_{min} moving in a bidimensional polygonal workspace $\mathcal{S}$, a sufficient condition for a path to be the solution of problem 1 is that it is a regular output of planner 1.*

Figure 2: Workspace (a) and corresponding 2D configuration space (b) illustrating Theorem 1.

Proof

The configuration space $\mathcal{V}$ associated with a circular robot contains C–obstacles that are generalized straight cylinders. In this case, the orientation parameter θ does not play a role in verifying holonomic constraints (4), nor does it influence the cost functional (1). Consider a two-dimensional configuration space $\mathcal{V}'$ where C–obstacles are built by isotropycally growing the obstacles in $\mathcal{S}$ by ρ. Fig.2 shows the workspace $\mathcal{S}$ (a) and the corresponding 2D configuration space $\mathcal{V}'$ (b) in a simple example.

Let P denote the set of free paths (i.e., triples $(x(\cdot), y(\cdot), \theta(\cdot))$ satisfying (4)) in $\mathcal{V}$, and P' be the corresponding set of $(x(\cdot), y(\cdot))$ pairs. Consider the visibility diagram V_d associated with $\mathcal{V}'$ (fig.3–a), and the modified diagram W_d (fig.3–b). The latter differs from V_d because two "phantom" circular obstacles of radius ρ and tangent to the initial direction at $\mathbf{q}_s$, and two analogous obstacles at $\mathbf{q}_g$, are considered (see fig.3–b). Start and goal phantom obstacles influence the visibility between two points only if either point is $\mathbf{q}_s$, respectively $\mathbf{q}_g$. Note that paths in V_d but not in W_d do not satisfy the constraint on curvature (6).

The BPD (and hence the EPD) built by the planner for the circular robot in $\mathcal{S}$ coincides with the modified visibility diagram W_d by construction. Therefore, if the path obtained on the EPD is regular (i.e., it contains no cusps), this is also the shortest path on W_d, and hence the shortest path in V_d subject to (6). From the properties of generalized visibility diagrams, the optimality of this path in P' subject to (6) follows. On the other hand, for every path in P' a corresponding path in P with $\theta(\tau) = \arctan\left[\frac{dy(\tau)}{d\tau}\left(\frac{dx(\tau)}{d\tau}\right)^{-1}\right]$ (where the indeterminacy of the arctan $(\cdot)$ function is solved by continuity) exists that satisfy the nonholonomic constraint (5). Such path is the optimal solution to Problem 1, and corresponds to the path obtained by the proposed planner. □

Figure 3: Extended visibility diagram without (a) and with "phantom" obstacles (b) for the example of fig. 2.

Figure 4: Impossibility to maneuver with too few obstacles.

3 Discussion

Theorem 1 is one of the first attempts in literature at solving the global optimal path planning problem (1). However, it only provides sufficient results for a particular vehicle. In this section we list some of the pitfalls of the proposed method along with simple heuristics that may help in applying the planner to more realistic robots.

Remark 1.
Note that only sufficiency results have been established because of two facts:

- If the planner results in a path that contains reversals, visibility graph arguments can not be applied in the proof. Piecewise optimality of paths between reversals can still be argued, but global path optimality remains unsolved;

- The method is not path–complete. For the circular robot of concern in theorem 1, incompleteness may be caused by the impossibility for the algorithm to maneuver in free space, except near the start and goal configurations. Consider for instance the case depicted in fig. 4, where the robot cannot reverse its direction along any path of the EPD, nor at the start and goal configurations (because of space limitations).

  A simple heuristic solution to this problem is to find a cell in free space where a Reeds/Shepp inversion pattern (see fig. 5–a) can be accomodated for, and to consider the corresponding additional pair of circles in the algorithm.

Figure 5: A Reeds/Shepp inversion pattern (a) can be introduced to solve the deadlock of fig 4 (b).

In building the Reeds/Shepp inversion pattern, existing circles are considered first, as this usually requires less clearance. In fig. 5–b, the problem in fig. 4 is solved. Notice that introduction of auxiliary circles produces a graph G' that includes the original graph G, hence the search on G' provides a path whose length is at least equal to the shortest path on G.

In fact, a characteristic of the proposed planner is its suitability to highly cluttered environments, where it accomplishes its best performance. The method's weaknesses are more evident when the scarceness of obstacles does not offer support to enough circles and, therefore, maneuver possibilities. An instance of such a problem is put into evidence by the parallel parking problem. In fact, the proposed algorithm can park a circular robot of radius R if the clearance is larger than three times R, while from the above mentioned controllability results we know that parking is theoretically possible in slots just larger than $2R$. There is probably no easy fix to this problem, as its solution is only possible by approximating a non–feasible trajectory with a very high number of nonholonomic maneuvers (this is actually what the method of Jacobs *et al.* [1990] does in this case). In cases when the proposed algorithm fails to find a path in narrow spaces, it is conceivable to employ it in a preliminary phase of "gross" planning, and switch to more time–consuming, path–complete planners for fine adjustements of the configuration.

Remark 2.
If $\rho_{min} \neq h$, the circular segments of BPD are drawn with radius $\rho = \max\{\rho_{min}, h\}$. If $\rho_{min} < h$, the algorithm is applied similarly, except for circles at the start and goal, that are drawn with radius ρ_{min}. The optimality properties of algorithm 1 are still retained in this case. Also Reeds/Shepp inversion patterns can be introduced, if necessary, using circles of radius ρ_{min}.

Figure 6: A possible deadlock for the algorithm

Figure 7: Modifications to the method to fix the deadlock in fig. 6

If $\rho_{min} > h$, path–completeness of the method is further reduced in cases such as that depicted in fig. 6,

where the vertex–to–vertex distance L is such that $2 * h < L < h + \rho_{min}$. An heuristic fix to this problem consists in replacing the circle drawn at each vertex with three circles of the same radius ρ_{min}. The center of the first circle lies on the bisector of the angle between the edges concurring in $\mathcal{X}_i$, at a distance $D = \rho_{min} - h$ from the vertex (see fig. 7–a). The centers of the second and third circles lie on the lines normal in $\mathcal{X}_i$ to the obstacle edges, at a distance $D = \rho_{min} - h$ (fig. 7–b). The rationale behind this heuristic is that the three circles approximate the envelope to the family of paths that "graze" the obstacle vertex. In fact, such envelope provides the shortest path on the extended visibility diagram (not necessarily the shortest bounded curvature path). Although such heuristic solution can not guarantee success in all cases, simulations showed that it can be usefully exploited in most situations.

Remark 3.

Remark 3.

For a vehicle of general shape, application of the proposed algorithm and heuristics does not guarantee *a priori* neither completeness nor optimality of paths. However, for polygonal vehicles whose aspect ratio is not too high (i.e., approximately "square" vehicles), qualitatively good results have been obtained in a number of simulations and experiments (see section 4). Note that the reference point for planning non–circular vehicles is assumed to be at the geometric center of its projection onto the plane. Consider for instance the simple planning problem for a Labmate in the environment depicted in fig. 8. The EPD obtained assuming $\rho_{min} = h$ is reported in fig. 8–a. Note that, due to the axial simmetry of the Labmate, all segments in EPD can be

Figure 8: Planning the path of a Labmate with different turning radii. a) EPD for $\rho_{min} = h$; b) corresponding path; c) path corresponding to $\rho_{min} = 1.5h$.

Figure 9: EPD (a) and final path (b) for the parallel–parking maneuver of a car–like vehicle.

followed either way. In fig. 8–b the corresponding shortest path on the EPD is shown. Finally, fig. 8–c shows the path resulting from application of the heuristic discussed in remark 2 in the case that $\rho_{min} = 1.5h$. Note that, in spite of the considerable increase of the minimum turning radius, the path is still very close to the intuitive optimum. The described path planner can also provide a solution for car–like robots, i.e. vehicles whose nonholonomic constraint equation involves the steering angle ϕ and is of the form

$$S(\mathbf{q})\dot{\mathbf{q}} = \begin{bmatrix} -\sin(\theta) & \cos(\theta) & 0 & 0 \\ -\sin(\theta+\phi) & \cos(\theta+\phi) & w\cos(\phi) & 0 \end{bmatrix} \begin{bmatrix} \dot{\mathbf{x}} \\ \dot{\mathbf{y}} \\ \dot{\theta} \\ \dot{\phi} \end{bmatrix} = 0$$

The EPD of a parallel parking maneuver is reported in fig. 9–a (orientation of segments is not shown). The parking maneuver provided seems very natural, as shown in fig. 9–b. More complex planning problems for a car–like vehicle are shown in fig. 10 and fig. 11. Note that, as compared to most current path planners, the proposed method behaves particularly well in much cluttered environments.

4 Experimental

Experimental verification of the practical feasibility of the proposed planner has been carried out in our laboratory using a LABMATE robot of Transition Research, Inc.. The LABMATE kinematics are those of a unicycle, and

Figure 10: EPD (a) and resulting path (b) for a car–like vehicle in a cluttered environment.

Figure 11: EPD (a) and resulting path (b) for a car–like vehicle in a corridor maze.

its driving inputs are the torques applied to two independent wheels. The shape of the vehicle is loosely square, centered in the middle of the wheel axle. The vehicle on–board control system implements tracking of lines and circles with sufficient accuracy if the velocity profile is smooth enough (errors are due mainly to odometric measurement inaccuracies caused by slippage at the wheels). The trajectories generated by our planner can thus be followed with ease by using LABMATE primitives. In order to accurately track planned trajectories, a Lyapunov–based closed loop control scheme has been employed, as described by Aicardi *et al.* [1994].

The goal of our experiments was to verify the preliminar feasibility of an "automatic valet parking" of car–like vehicles in both a front and parallel parking lot. To this purpose, the shape of the LABMATE has been modified to resemble that of a car (in scale, approx. $80 \times 160cm$), and software has been written to implement a bound on the minimum turning radius of the vehicle (set to 40 cm). Detection of obstacles has been realized by using a set of US detectors available with the vehicle. US images are pre–processed and sent to the host computer (an Intel–486 based PC), via a radio serial link at 9600 baud. The host computer builds a simple 2D depth map of the scene and updates it while the vehicle moves down the parking lot corridor looking for a vacant slot. When room enough to maneuver the vehicle into is found, the planner process is started on the salient features of the map, and the resulting plan is executed directly after. In fig. 12 an experiment on front parking is described by the temporal sequence of phases. The updating of the experimental depth map superimposed to a picture of the actual environment configuration is shown in fig. 12 (a) through (c). It can be noted that

sensor readings are rather accurate, except for a certain number of outliers, which have been taken care of by suitable processing. Fig. 12 (d) illustrates the construction of the EPD, while fig. 12 (e) shows the resulting parking maneuver. In fig.12 (f) the tracking error between the planned path and the trajectory actually followed by the Labmate is reported. Fig. 13 represents an analogous sequence for a parallel parking maneuver. The planning phase of these experiments took less than 2 seconds, while the complete parking detection, planning, and execution took about 2 minutes. This was mainly due to the necessity of proceeding very slowly in the detection phase to avoid excessive errors from the US sensors, and also slippage of wheels. The sensorial equipment of the vehicle resulted as one of the most critical components in the experiment. On the overall, the above reported experimental results confirmed the suitability of the proposed planner to real–time applications in near–future intelligent cars.

5 Conclusion

In this paper we have discussed a planning algorithm for nonholonomic, bounded curvature path planning among obstacles whose output is the shortest feasible regular path for a particular vehicle. Although the proposed method is not complete, nor its optimality properties are trivially carried over to more general vehicles, very reasonable paths are generated by using only a few additional simple heuristics.

As compared with other methods known in the literature, the proposed planner does not need to build a supporting free path by means of configuration space methods nor does it require discretization of the configuration space. Paths generated by our method are typically very simple concatenations of Reeds/Shepp paths. An important quality of the proposed method is that it can be easily implemented even in cluttered workspaces, where the method actually performs comparatively best.

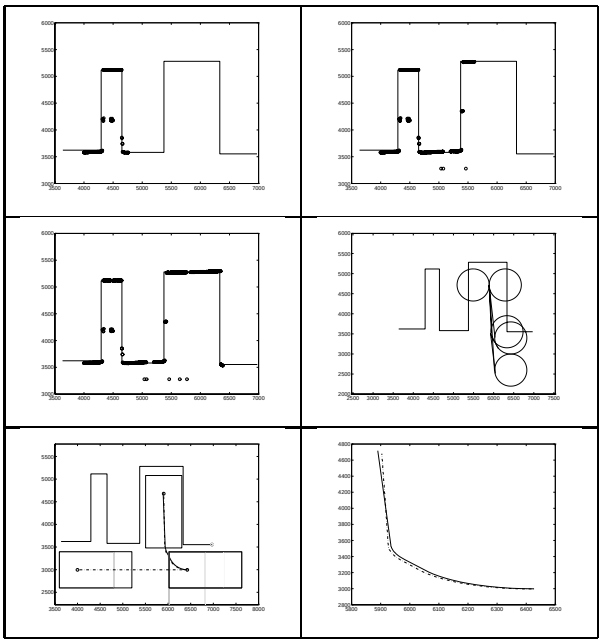

Figure 12: Sequence describing an experimental automated front parking maneuver. (a), (b), (c): US sensor signals are used to build a depth map of the parking lot as the vehicle scans the row; (d): Emended Path Diagram built by the planner; (e): parking maneuver; (f): planned path (solid) and actual trajectory (dashed).

References

M. Aicardi, G. Casalino, A. Balestrino, A. Bicchi: "Closed loop smooth steering of unicycle–like vehicles", Proc. 33rd Proc. Conf. on Decision and Control, pp. 2455–2458, 1994.

J. Barraquand, J.C. Latombe: "On nonholonomic mobile robots and optimal maneuvering", Proc. 4th Int. Symposium of Intelligent Control, Albany, NY, 1989.

J. Barraquand, J.C. Latombe: "Controllability of Mobile Robots with Kinematic Constraints", Technical Report No. STAN–CS–90–1317, Dept. of Computer Science, Stanford University, 1990.

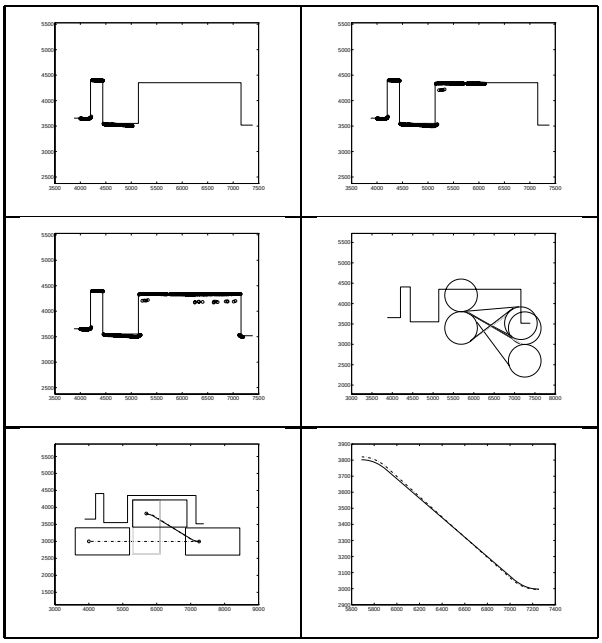

Figure 13: Sequence describing an experimental automated parallel parking maneuver. (a), (b), (c): US sensor signals are used to build a depth map of the parking lot as the vehicle scans the row; (d): Emended Path Diagram built by the planner; (e): parking maneuver; (f): planned path (solid) and actual trajectory (dashed).

J.D. Boissonnat, A. Cerezo, and J. Leblond: "Shortest Paths of Bounded Curvature in the Plane", Proc. IEEE Int. Conf. on Robotics and Automation, pp.2315–2320, 1992.

A. E. Bryson, and Y. Ho: "Applied Optimal Control", Hemisphere Publ. Co, 1975.

L. E. Dubins: "On curves of minimal length with a constraint on average curvature and with prescribed initial and terminal positions and tangents", American Journal of Mathematics, vol.79, pp.497–516, 1957.

S. J. Fortune, G. T. Wilfong: "Planning constrained motion", Proc. 4th ACM Symposium on Computational Geometry, pp. 445–459, 1988.

P. Jacobs, J. Canny: "Planning Smooth Paths for Mobile Robots", *IEEE International Conference on Robotics and Automation*, AZ, 2–7, 1989.

P. Jacobs, J. P. Laumond, M. Taix and R. Murray: "Fast and Exact Trajectory Planning for Mobile Robots and Other Systems with Nonholonomic Constraints", Technical Report 90318, LAAS/CNRS, Toulouse, France, September 1990.

J–C. Latombe: "Robot Motion Planning", Kluwer Academic Publishers, 1990.

J. P. Laumond: "Feasible Trajectories for Mobile Robots with Kinematic and Environment Constraints", Proc. International Conference on Intelligent Autonomous Systems, Amsterdam, 346–354, 1986.

B. Mirtich, J. Canny: "Using Skeletons for Nonholonomic Path Planning among Obstacles", *IEEE International Conference on Robotics and Automation*, pp. 2533–2540, May 1990.

S. Monaco, and D. Normand–Cyrot: "An Introduction to Motion Planning under Multi–Rate Digital Control", Proc. Conf. on Decision and Control, 1992.

R. Murray and S.S. Sastry: "Nonholonomic Motion Planning: Steering Using Sinusoids", IEEE Trans. Automatic Control, vol.38, no.5, pp.:700–716, May, 1993.

L.S. Pontryagin, V.G. Boltyanskii, R. V. Gamkrelidze, and E. F. Mishchenko: "The Mathematical Theory of optimal Processes", Interscience pub., 1962.

J. A. Reeds, R. A. Shepp: "Optimal Paths for a Car that Goes both Forward and Backward", Pacific Journal of Mathematics, vol. 145(2), 1990.

H. J. Sussmann and G. Tang: "Shortest Paths for the Reeds–Shepp Car: a Worked Out Example of the Use of Geometric Techniques in Nonlinear Optimal Control", SYCON report 91–10, 1991.

List of Captions for Figures

1. A generic car–like robot (a) and a particular unicycle vehicle (b).
2. Workspace (a) and corresponding 2D configuration space (b) illustrating Theorem 1.
3. Extended visibility diagram without (a) and with "phantom" obstacles (b) for the example of fig. 2.
4. Impossibility to maneuver with too few obstacles.
5. A Reeds/Shepp inversion pattern (a) can be introduced to solve the deadlock of fig 4 (b).
6. A possible deadlock for the algorithm.
7. Modifications to the method to fix the deadlock in fig. 6.
8. Planning the path of a Labmate with different turning radii. a) EPD for $\rho_{min} = h$; b) corresponding path; c) path corresponding to $\rho_{min} = 1.5h$.
9. EPD (a) and final path (b) for the parallel–parking maneuver of a car–like vehicle.
10. EPD (a) and resulting path (b) for a car–like vehicle in a cluttered environment.
11. EPD (a) and resulting path (b) for a car–like vehicle in a corridor maze.
12. Sequence describing an experimental automated front parking maneuver. (a), (b), (c): US sensor signals are used to build a depth map of the parking lot as the vehicle scans the row; (d): Emended Path Diagram built by the planner; (e): parking maneuver; (f): planned path (solid) and actual trajectory (dashed).
13. Sequence describing an experimental automated parallel parking maneuver. (a), (b), (c): US sensor signals are used to build a depth map of the parking lot as the vehicle scans the row; (d): Emended Path Diagram built by the planner; (e): parking maneuver; (f): planned path (solid) and actual trajectory (dashed).

List of Footnotes

1. Manuscript received . The Authors are with the Centro "E. Piaggio" and Dipartimento di Sistemi Elettrici e Automazione, Università di Pisa, Italia. This work was supported in part by the C.N.R. - Progetto Finalizzato Robotica Grants 93.01079.PF67 and 93.00880.PF67.